South African Journal of Botany 127 (2019) 147–152

Contents lists available at ScienceDirect

South African Journal of Botany

journal homepage: www.elsevier.com/locate/sajb

Assessment of algal biomasses having different cell structures for biosorption properties of acid red P-2BX dye

Ü.D. Gül[a,*], B.E. Taştan[b,c], G. Bayazıt[d]

[a] Vocational School of Health Services, Biotechnology Application and Research Center, Bilecik Seyh Edebali University, 11230 Bilecik, Turkey
[b] Vocational School of Health Services, Gazi University, 06830 Ankara, Turkey
[c] Polatlı Faculty of Science & Arts, Ankara Hacı Bayram Veli University, 06900 Ankara, Turkey
[d] Department of Biotechnology, Bilecik Seyh Edebali University, 11230 Bilecik, Turkey

ARTICLE INFO

Article History:
Received 10 March 2019
Received in revised form 20 August 2019
Accepted 29 August 2019
Available online 14 September 2019

Edited by WA Stirk

Keywords:
Acid red P-2BX
Biomass
Biosorption
Phormidium animale
Scenedesmus sp

ABSTRACT

The increased applications of synthetic dyes in the textile industrial activities have negative implications such as water pollution by dye containing effluents. The treatment of industrial wastewater is important due to the toxic effects of dyes. Biosorption is defined as a relatively economical and eco-friendly wastewater treatment method. The aim of this study was to examine the biosorption of Acid Red P-2BX (ARP-2BX) dye that is extensively used and abundantly found in textile wastewater. The dye biosorption capacities of prokaryotic algae (*Phormidium animale*) and eukaryotic algae (*Scenedesmus* sp.) were investigated. The effects of pH (2–10), biosorbent type (ash or dried), initial dye concentration, biosorbent dosage, contact time and temperature were determined. Maximum dye removal was performed by dried *P. animale* as 99.70 ± 0.27%. The biosorption isotherms and kinetics were also calculated, the ARP-2BX dye biosorption was fitted with Langmuir isotherm and pseudo-second-order kinetic models. In order to analyze the changes that occurred in algal structure, FTIR and elemental analysis were done. The results of this study concluded that *P. animale* was a favorable biosorbent for treatment of textile wastewater.

1. Introduction

Textile wastewater contains a high amount of synthetic dyes which are extensively used to dye textile products (Yaseen and Scholz, 2018). The high concentrations of dyes are discharged to water resources from the textile effluents and, then pollute the aquatic environments (Chia and Musa, 2014). Removal of these dyes from water is an important process to protect aquatic organisms.

Biosorption is a wastewater treatment process using organisms such as algae, bacteria or fungi due to their special surface properties (Aksu and Tezer, 2005). Many metabolism-independent processes (chelation, physical adsorption, ion exchange, chemical adsorption, and complexation) which take place in the cell wall of these organisms have important roles in biosorption (Aksu and Tezer, 2005). It is a preferred mechanism because provides cheap, selective, efficient, and successful removal performance. It is also advantageous to use dead microbial cells in this process because they are not affected by the toxicity of the pollutants, do not required nutrient supplementary and do not need special storage conditions. The pollutant sorption performance of dead cells is similar or greater than growing and resting cells (Aksu and Tezer, 2005).

The interactions which are important for the efficiency of biosorption, between dyes and microorganisms are related to the chemical structure of dye and surface properties of microorganism (Mnif et al., 2015). Environmental conditions such as pH, initial dye concentration, biosorbent dosage and contact time also affect the success of the biosorption process (Mnif et al., 2016).

Algae are single-cell organisms living in aqueous environments and most of the algal biomasses were found in wastewater (Renuka et al., 2014). Recent studies are interested in usage of algae for removal of textile dyes from dye-containing water (Lim et al., 2010; Mona et al., 2011; Dotto et al., 2013; Elumalai and Saravan, 2016; Preeti and Veena, 2017; Omar et al., 2018). However, there is no comparative assessment of biosorbent properties of a prokaryotic and eukaryotic algal biomass. In this study the biosorption performance of a prokaryotic algae, namely *Phormidium animale* and eukaryotic algae namely, *Scenedesmus sp.* were compared. In this study the biosorption performance of a prokaryotic algae, namely *Phormidium animale* and eukaryotic algae namely, *Scenedesmus* sp. were compared. The optimal environmental conditions and changes in the surface properties of the most effective biosorbent were also determined. The biosorption isotherms, kinetics and, the changes in the elemental structure of biosorbent before and after the biosorption process were investigated in the current study.

* Corresponding author.
E-mail address: ulkuyedudu.gul@bilecik.edu.tr (Ü.D. Gül).

https://doi.org/10.1016/j.sajb.2019.08.047
0254-6299/

2. Materials and methods

2.1. Preparation of dye solution

Acid Red P-2BX (ARP-2BX) dye was obtained from the textile factory in Turkey. The structure of ARP-2BX is given in Fig. 1. The stock solution was prepared as 1000 mg/L in distilled water. The working solutions of ARP-2BX were prepared by diluting the stock solution to the desired concentrations (showed as C_o (mg/L) in tables and figures) in each experiment. The desired amount of dye solutions were added to the Erlenmeyer flasks at known initial pH value for the biosorption experiments.

2.2. Microorganisms and culture conditions

Scenedesmus sp. was newly isolated from Eskişehir, Turkey (Tastan and Tekinay, 2016) and *Phormidium animale* were isolated from Çanakkale, Turkey (Culture Collection of Microalgae, Vocational School of Health Services, Gazi University, Ankara, TURKEY). *Scenedesmus* sp. is a member of eukaryotic green algae. *Phormidium animale* is a prokaryotic blue-green algae. Incubation of microalgae was carried out in 100 mL of BG 11 culture media in 250 mL Erlenmeyer flasks at 25 ± 2 °C at 48 μmol/m^2 s (2400 lx) (Rippka, 1988). The pH of the culture media was adjusted with concentrated (1 M) and dilute (0.01 M) sulfuric acid/sodium hydroxide solutions.

Subsequently, a large volume of biomass production was carried out in BG11 medium in 5 L of plastic sterile containers. The sterilization was performed with dilute sodium hypochlorite and/or ethanol solutions. Continuous air was applied to the containers with aquarium motors. The motors have a working capacity of 8 W with 2–4 outputs.

Growth curves were prepared from cell density data obtained with a spectrophotometer at every other day during 30 days.

The specific growth rate was calculated from Eq. (1) (Ip and Chen, 2005);

$$\mu = \ln x_2 - \ln x_1 / t_2 - t_1 \quad (1)$$

where X_2 and X_1: dry cell weight concentrations (g/L) at time t_2 and t_1, respectively.

Scenedesmus sp. and *P. animale* were harvested at 15th and 20th days of incubation, respectively. After the completion of the logarithmic growth phase for both of the algae, the algal biomasses were harvested from the media by centrifugation (6000 rpm, 5 min, 25 ± 2 °C) and were dried at 70 °C for overnight in aluminum beakers and, then homogenized and ground to a powder form. The powder was passed through a sieve (0.5 mm) and used in the biosorption experiments.

2.3. Biosorption studies

All of the biosorption experiments were performed in Erlenmeyer flasks containing 100 mL working solution with desired amounts of ARP-2BX dye. The effect of pH was determined at different pH values of 2, 4, 6, 8 and 10. The flasks contained only dye and working solutions were used as a control. The two types of biosorbent such as dried and ash were used in this study. The ash biosorbent was prepared by drying the algal biomass in the ash oven at 500 °C for 30 min. In order to compare biosorbent type (dried and ash), dye-containing solutions were prepared including 1 g/L of each biosorbent (dried and ash). The effect of contact time (30–1440 min), initial dye concentration (57.14, 91.71 and 139.57 mg/L), temperature (25, 35 and 45 °C) and biosorbent dosage (1, 2 and 4 g/L) were examined in batch scale level. The effect of biosorbent dosage on dye biosorption capacity of dried *P. animale* experiments was carried out in flasks contained working solutions at pH 2 with 91.71 mg/L dye concentrations. The amounts of biosorbent dosages were varied as 1, 2 and 4 g/L. The effects of temperature and contact time on dye removal of dried *P. animale* were tested in the same experimental studies at 25, 35 and 45 °f and the samples were taken from 30 to 1440 min.

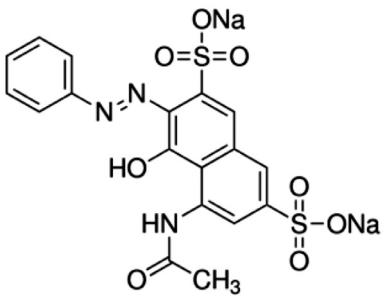

Fig. 1. The structure of ARP-2BX

All of the experiments were performed in triplicate. The standard error of data was calculated according to Eq. (2) (Kenney and Keeping, 1951);

$$SE = \sqrt{\sigma^2} \quad (2)$$

where σ represents the square root of the estimated error variance of the quantity. SPSS 17 was applied to analyze the data and ANOVA (one-way) was used to compare average values. Correlation coefficients were calculated by using the Microsoft Excel package.

2.4. Analytical methods

ARP-2BX dye concentration in the supernatant was determined spectrophotometrically (Labomed INC. 22 model spectrophotometer). The concentration of ARP-2BX was determined by measuring the absorbance at 535 nm, which was the wavelength of observing the maximum absorption peak for dye.

For analysis, 2 mL of samples were taken at definite times from the working solution that contained the microorganism and dye. The samples were centrifuged (Hettich EBTA12 model centrifuge) at 4000 rpm for 3 min and the supernatant was used for dye analysis after appropriate dilutions.

The dye removal percentage was calculated from Eqs. (3) and (4);

$$BR(\text{Biosorption Rate}\%) = (C_o - C_f)/C_o \times 100 \quad (3)$$

The uptake of dye by unit mass of biosorbent at any time (q_m:mg/g) was determined from;

$$q_m = C_o - C_f / X_m \quad (4)$$

where C_o, C_f and X_m represent initial dye concentration (mg/L), the final dye concentration at any time (mg/L) and the sorbent concentration (g/L), respectively.

2.5. Biosorption isotherms and kinetics

This experiment was also applied to investigate the isotherm studies by fitting the data with the most commonly used isotherm models as Langmuir, Freundlich, and Dubinin-Radushkevich (D-R). The Langmuir and Freundlich isotherm equations are given in Eqs. (5) and (6), respectively;

$$C_e/q_e = (1/q_m)C_e + 1/K_L q_m \quad (5)$$

Langmuir Isotherm (Langmuir, 1918).

$$\ln(q_e) = \ln(K_F) + 1/n \ln(C_e) \quad (6)$$

Freundlich Isotherm (Freundlich, 1906) where C_e, q_e q_m, K_L and K_F represent the equilibrium concentration of adsorbate (mg/L), the amount of dye adsorbed per unit weight of adsorbent at equilibrium (mg/g), the maximum capacity of adsorption (mg/g), Langmuir

isotherm constant (L/mg) and Freundlich isotherm constant (L/mg), respectively.

The Dubinin-Radushkevich (D-R) equality is given in Eq. (7);

$$Q = X_{DR} e^{-K_{DR}\varepsilon^2} \quad (7)$$

where Q, X_{DR}, K_{DR}, ε, and R represent the amount of adsorbed Pb^{2+} (mol kg^{-1}), a measure of adsorption capacity, activity coefficient (mol^2 K J^2), Polanyi potential and the ideal gas constant (8.314 J mol^{-1} K^{-1}), respectively.

Polanyi potential is calculated from Eq. (8);

$$\varepsilon = RT \ln\left(1+\frac{1}{c_e}\right) \quad (8)$$

where R and T (K) represent the ideal gas constant (8.314 J mol^{-1} K^{-1}) and the absolute temperature, respectively.

Adsorption free energy (E) (kJ mol^{-1}) is calculated by Eq. (9);

$$E = (2K_{DR})^{-0.3} \quad (9)$$

Different types of mathematical equations about kinetic biosorption data can be used to examine the dynamics of the biosorption process in terms of the theoretical q_e values and order of rate constant. Kinetic data were calculated with the equations of pseudo-first-order and pseudo-second-order kinetic models. Eqs. (10) and (11) were used to obtain pseudo-first-order and -second-order kinetic data.

$$\log(q_e - q_t) = -k_1/2.303t + \log q_e (\text{Pseudo–first–order kinetic model}) \quad (10)$$

$$t/q_t = 1/k_2 q_e^2 + 1/q_e . t (\text{Pseudo–second–order kinetic model}) \quad (11)$$

where q_e, q_t, k_1 and k_2 represent the amounts of dye adsorbed at equilibrium (mg/g), the amounts of dye adsorbed at time t (mg/g), rate constant of pseudo-first-order kinetic model and rate constant of pseudo-second-order kinetic model, respectively.

2.6. FTIR analysis

FTIR was recorded using Agilent Technologies, Cary 630 FTIR spectrophotometer. The dried algal biomass, obtained before and after biosorption, were ground into powders, blended with dry spectroscopic grade powders, and pressed into small disks for FTIR measurements. Samples were scanned at the scan range of 400–4000 cm^{-1}.

2.7. Elemental analysis

LECO CHNS 628 organic elemental analyzer was used for elemental analysis of ARP-2BX dye and dried *P. animale* biomasses with and without dye loaded.

3. Results

3.1. The effect of pH, algal strain, and biosorbent type

The dye biosorption rates by both dried and ashed *Scenedesmus* sp. were increased from pH 2 to 8 and decreased at pH 10. Dried *Scenedesmus* sp. removed 8.90 ± 0.40% and 12.91 ± 0.51% at pH 2 and 8, respectively. Ash *Scenedesmus* sp. performed 10.60 ± 1.52% and 14.75 ± 3.33% dye biosorption rate at pH 2 and 8, respectively (Table 1). Both types of *Scenedesmus* sp. biosorbents (dried and ashed) showed maximum dye removal at pH 8. In addition to this, ashed *Scenedesmus* sp., showed higher dye removal rate than dried *Scenedesmus* sp. (Table 1).

Dried *P. animale* showed 89.72 ± 0.77% and 2.86 ± 2.82% dye removal percentage at pH 2 and 8, respectively. Ashed *P. animale* removed 20.76 ± 3.43% and 1.35 ± 0.84% of dye at pH 2 and 8, respectively (Table 1). Both of the *P. animale* biosorbent types (dried and ash) showed maximum dye biosorption rates at pH 2. In addition to this, dried biosorbent of *P. animale* performed more effective biosorption than ashed one.

Table 1
The effect of pH, algal strain and biosorbent type at 25 °C. Values given are mean of n samples ± S.D., where n = 2.

Biosorbent	Type	pH	C_o (mg/L)	C_e (mg/L)	BR (%)
Scenedesmus sp.	Dried	2	102.71	93.57	8.90 ± 0.40
Scenedesmus sp.	Dried	4	102.57	91.86	10.44 ± 1.82
Scenedesmus sp.	Dried	6	102.57	91.43	10.86 ± 1.62
Scenedesmus sp.	Dried	8	105.14	91.57	12.91 ± 0.51
Scenedesmus sp.	Dried	10	133.00	121.00	9.02 ± 0.10
Scenedesmus sp.	Ashed	2	102.43	91.57	10.60 ± 1.52
Scenedesmus sp.	Ashed	4	101.86	92.86	8.84 ± 1.01
Scenedesmus sp.	Ashed	6	108.43	93.00	8.95 ± 1.01
Scenedesmus sp.	Ashed	8	105.57	90.00	14.75 ± 3.33
Scenedesmus sp.	Ashed	10	100.43	88.57	11.81 ± 0.10
P. animale	Dried	2	91.71	9.43	89.72 ± 0.77
P. animale	Dried	4	88.14	52.86	40.03 ± 6.18
P. animale	Dried	6	90.29	89.57	0.80 ± 3.53
P. animale	Dried	8	99.86	97.00	2.86 ± 2.82
P. animale	Dried	10	91.57	91.63	0.07 ± 3.23
P. animale	Ashed	2	97.71	77.43	20.76 ± 3.43
P. animale	Ashed	4	96.57	80.43	16.71 ± 4.14
P. animale	Ashed	6	92.57	92.00	1.62 ± 1.21
P. animale	Ashed	8	95.43	94.14	1.35 ± 0,84
P. animale	Ashed	10	95.14	94.00	1.20 ± 0,60

*BR: Biosorption rate.

There were no significant changes in the control flasks contained dye and working solutions at different pH values (2, 4, 6, 8 and 10). According to the results of these experimental studies, the dried *P. animale* biosorbent at pH 2 was selected to use in the continuous experiments.

3.2. The effect of initial dye concentration

In order to determine the effect of initial dye concentration on biosorption rate of dried *P. animale* biosorbent, different values of dye concentrations such as 57.14, 91.71, 139.57 and 147.29 mg/L were tested in flasks contained working solutions with pH 2. Increasing dye concentration from 57.14 to 147.29 mg/L decreased dye removal performance from 98.50 ± 0.88% to 29.97 ± 1.67%, respectively (Table 2).

3.3. The effect of biosorbent dosage

The increment of biosorbent (dried *P. animale*) dosage (up to 4 g/L) resulted in augmentation of biosorption rate up to 97.35 ± 0.65% (Fig. 2).

3.4. The effect of temperature and contact time

Dye biosorption rates increased with time. Maximum dye biosorption rate occurred at the minute of 1440 and there was no significant change after 1440 min at all temperature values. The dye

Table 2
The effect of dye concentration at T: 25 °C. Values given are mean of n samples ± S.D., where n = 2.

Biosorbent	Type	pH	C_o (mg/L)	C_e (mg/L)	BR (%)
P. animale	Dried	2	57.14	0.86	98.50 ± 0.88
P. animale	Dried	2	91.71	9.43	89.72 ± 0.77
P. animale	Dried	2	139.57	47.00	66.33 ± 1.48
P. animale	Dried	2	147.29	103.14	29.97 ± 1.67

*BR: Biosorption rate.

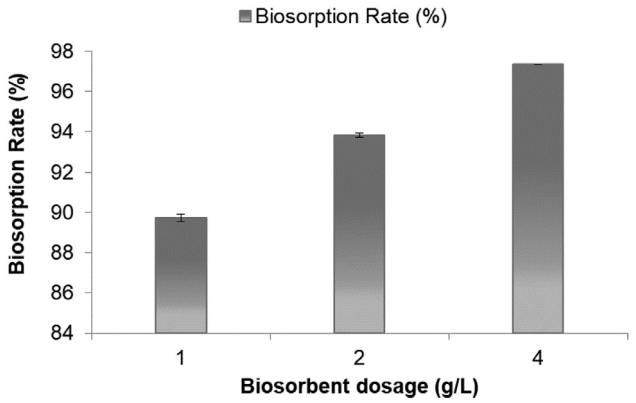

Fig. 2. The effect of biosorbent dosage at pH 2 with 91.71 mg/L dye concentrations. Different letters indicate significant differences (p = .05, df = 2). Error bars represent the standard error of the mean.

biosorption rates were calculated as 89.72 ± 0.77%, 96.50 ± 0.50 and 99.70 ± 0.27 at 25, 35 and 45 °C, respectively (Fig. 3).

3.5. FTIR analysis results

The FTIR analysis was done with the samples obtained from the experiments before and after the biosorption process at optimal conditions. The peaks at 1438 vs 1230 cm^{-1} occurred after the biosorption process. And also, a new peak formation at 1230 cm^{-1} was appeared after biosorption (Fig. 4).

3.6. Biosorption isotherms and kinetics

Biosorption isotherms and kinetics were calculated at optimal conditions. The correlation values of Langmuir and Freundlich isotherms were calculated as 0.999 and 0.967 for the biosorption of ARP-2BX dye on dried *P. animale*, respectively. Also, the adsorption energy from the D-R model was found to be 7.36 kJ mol^{-1} (Table 3 a).

The correlation of the pseudo-first-order model was high as 0.978 but the experimental qe_{exp} value was different from calculated qe_{cal}. For the pseudo-second-order model, both the correlation was high as 0.997 and the experimental and calculated *qe* values were very close.

3.7. Elemental analysis

After biosorption of the Acid Red P-2BX dye by *Phormidium animale*, the amounts of Carbon, Hydrogen, and Nitrogen were increased in the algal biomass while the amount of Oxygen decreased (Table 4).

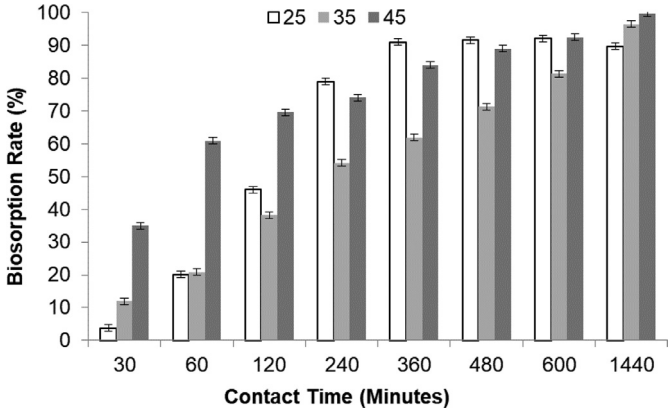

Fig. 3. The effect of temperature and contact time at pH 2 with 91.71 mg/L dye concentrations. Different letters indicate significant differences (p = .05, df = 2). Error bars represent the standard error of the mean.

In this case, it was considered that oxygen was lost during the biosorption process.

3.8. Statistical analysis

According to the results of statistical calculations, the parameters were accepted as meaningful; the tested factors (pH, temperature, biosorbent dosage) a significant effect on dye biosorption ($p < .05$). The statistical analysis showed that the effect of pH on dye biosorption by *Scenedesmus* sp. was not statistically meaningful ($p > .05$). On the other hand, the pH has a significant effect on color removal by *P. animale* ($p < .05$).

4. Discussion

The results of pH experiments showed the biosorption rate of ARP-2BX textile dye by algal biosorbent changed depending on the cell structure of algal strain (prokaryotic and eukaryotic) and the type of biosorbent (dried and ash). The optimal pH for dye biosorption of *Scenedesmus* sp. (eukaryotic) and *P. animale* (prokaryotic) were different, being 8 and 2, respectively. An increase of pH from 2 to 8 increased dye biosorption by both types of (dried and ash) *Scenedesmus* sp. biosorbents. A further increase of pH from 8 to 10 resulted in a significant decrease in biosorption rates. It was assumed that above pH 8, there were some changes in the solution depending on the protons transferring from the biosorbent (Tunalı Akar et al., 2016). Also, the ash *Scenedesmus* sp. biosorbent showed a better dye removal rate than dried *Scenedesmus* sp., In contrast, ashed *P. animale* biosorbent had lower dye removal biosorption rate than the dried biosorbent

Scenedesmus sp. is a eukaryotic green microalga and its adsorption properties are related to the proteins found in the outer site of the cell wall (Chen et al., 2014). The functional groups on the surface of *Phormidium* sp. had a significant role on the biosorption of phenol by the microalgal biosorbent at low pH values (Ertuğrul Karatay et al., 2017). In the present study, the dye biosorption capacities of *Scenedesmus* sp. (ashed) and *P. animale* (dried) were calculated as 15.57 and 82.28 mg/g, respectively. Due to this maximum dye removal capacity dried *P. animale* was selected for further experiments. Ashed and dried *P. animale* biosorbents showed maximum dye biosorption rates at pH 2 as 20.76 ± 3.43% and 89.72 ± 0.77%, respectively (Table 1). When comparing the dye biosorption rates of dried and ashed *P. animale*, the dried biosorbent had four times more dye removal rate (Table 1). Also while the pH values increased from 2 to 10, the biosorption rates were sharply decreased from 89.72 ± 0.77% to 0.07 ± 3.23%. Similarly, the increment of pH values from 2 to 6 resulted in a sharp decline in Reactive Red 198 dye biosorption rates by a cyanobacterium (prokaryotic blue-green algae) *Nostoc linckia* HA 46 (Mona et al., 2011). The chromophore group of reactive dyes has a negative electrical nature and at low pH values due to the positive nature of the algal surface, powerful electrostatic interactions occur between the reactive dye molecules and the surface of algae (Ozer et al., 2005). Therefore, these interactions tend to enhance the adsorption of dye ions on to the positive charged algal surface. In the present study, optimal pH value for Acid Red P-2BX biosorption by dried *P. animale* was determined as 2.

Initial dye concentrations ensure a significant force to handle with mass transfer resistance of dye molecules between aqueous and solid phases (Aravindhan et al., 2007). In the present study, the dye biosorption rates declined by increasing initial dye concentrations (Table 2). Increasing dye concentration provided the saturation of the active groups on the surface of the algae and after saturation there was no active site on the biosorbent to interact with dye molecules. This situation resulted in declining of dye biosorption rate (Mane et al., 2010). Similarly, higher dye concentrations resulted in reducing of dye removal rates by algal biomasses such as removal of reactive

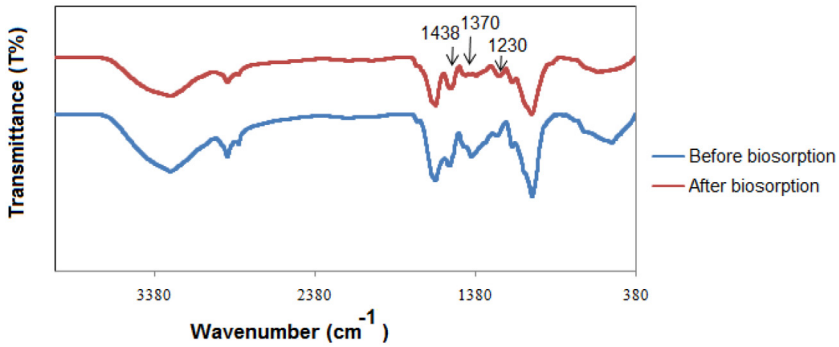

Fig. 4. FTIR spectrum of *P. animale* before and after ARP-2BX dye biosorption

dyes by *Chlorella vulgaris* (Aksu and Tezer, 2005), basic yellow dye by *Caulerpa scalpelliformis* (Marungrueng and Pavasant, 2006), reactive red 120 by *Spirogyra majuscule* (Celekli et al., 2009), and Reactive Red 198 by *Nostoc linckia* HA 46 (Mona et al., 2011).

Biosorbent dosage also affected the adsorption process by means of active sites on the biosorbent. Increasing in the dye removal with biosorbent dosage can be attributed to an increase in biosorption surface area and the presence of more active adsorption site. It was possible to increase biosorption capacity by increasing the amount of biosorbent Kousha et al., 2012). Increasing biosorbent dosage of algal biomasses (*U. reticulata*, *S. crassifolium*, and *G. corticata*) from 0.5 to 2 g/L, the dye biosorption rates were raised up (Omar et al., 2018). The augmentation of algal biosorbent dosage resulted in increasing of biosorption rate according to the results of the current study.

Temperature is another parameter that affects the biosorption rate. The biosorption rate increased with increasing temperature due to the increment of active binding sites on the surface of biosorbent for dye adsorption (Mona et al., 2011). The biosorption rate of ARP-2BX dye by dried *P. animale* increased to 99.70 ± 0.27% with the increment of temperature up to 45 °C after 1440 min (Fig. 3). A sharp increase was observed in adsorption % after 240 min, indicated the approaching of equilibrium time. Sadegh et al., 2017 reviewed the performance of low cost adsorbents including agricultural wastes, industrial solid wastes, biomass, clay minerals, and zeolites and concluded that when the adsorption process was close to the equilibrium time the increment of adsorption was observed. The optimal times for dye biosorption by dried *P. animale* biosorbent were found 360 min at 25 °C and 1440 min at 35 and 45 °C. The contact time also influences total biosorption capacity. Increment of contact time up to optimum time for biosorption increases dye removal after which the biosorption rate becomes relatively constant (Bilal et al., 2018).

The FTIR results indicated that new peak formations at 1438, 1370 and 1230 cm^{-1} occurred after dye biosorption. Peaks at 1500–1400; 1400–1290 and 1250–1020 cm^{-1} represent C–C stretching vibration presence of aromatics, N–O stretching vibration presence of nitro compounds and C–N stretching vibration presence of aliphatic amines, respectively (Theivandran et al., 2015). The changes appeared in the FTIR spectrum between before and after biosorption of dye indicated the interactions of adsorbate with the active sites of adsorbents (Michalak et al., 2013; Salvi and Chattopadhyay, 2017).

In the present study, the biosorption was fitted with the Langmuir isotherm model because of the highest correlation value. The q_m value (100 mg/g) indicating the biosorption capacity from the Langmuir constants and the K_L value indicating the biosorption energy, were found to be K_L = 1.11 L/mg (Table 3 a). Similarly, the azo dye biosorption by *Spirulina platensis* was compatible with the Langmuir isotherm model (Dotto et al., 2013). This model indicates the homogeneous surface of the biosorbent covered with a single layer.

The calculations of kinetic models showed that the ARP-2BX dye biosorption on the dried *P. animale* was compatible with the pseudo-second-order kinetic model (Table 3 b). Similarly, the biosorption kinetic model of all Remazol dyes (Remazol Black B, Remazol Red RR, and Remazol Golden Yellow RNL) on dried *Chlorella vulgaris* was suitable with pseudo-second-order model (Aksu and Tezer, 2005). The E obtained from D–R models' calculations, indicates the mechanism of adsorption such as physical or chemical. $8 < E < 16$ indicates the adsorption is chemically controlled and while $E < 8$ kJ mol^{-1} reveals the adsorption proceeds physically (Helfferich, 1962). According to the D–R model results of the current study, the adsorption energy from the D–R model was found to be 7.36 kJ mol^{-1}, which indicated that the biosorption process was physical.

5. Conclusion

The use of *P. animale* and *Scenedesmus* sp. as biosorbent for biosorption of Acid Red P-2BX was studied. The effects of pH (2–10), biosorbent type (ash or dried), initial dye concentration (57.14–147.29 mg/L), biosorbent dosage (1–4 g/L), contact time (30–1440 min) and temperature (25–45 °C) were determined. For *Scenedesmus* sp., the optimal biosorption activity of both biosorbent types occurred at pH 8 and the ashed biosorbent performed more effectively than the dried biosorbent. *P. animale* showed maximum dye sorption at pH 2. While comparing the dye biosorption rates of dried and ashed *P. animale*, the dried biosorbent had four times more

Table 3
(a) Langmuir, Freundlich and D-R constants for ARP-2BX biosorption by dried algal biosorbent (b) Kinetic parameters for the biosorption of ARP-2BX onto dried *P. animale* biosorbent

a. Isotherm models

Langmuir		Freundlich		Dubinin-Radushkevich	
q_{max} (mg/g)	100	K_F	58.62	X_{DR}	32.16
K_L	1.11	1/n	0.127	$-K_{DR}x10^9$	8.944×10^{-9}
R^2	0.999	R^2	0.967	R^2	0.982
				E/kJ mol^{-1}	7.36

b. Kinetic models

Pseudo-first-order model		Pseudo-second-order model	
qe_{cal}	1.482	qe_{cal}	62.50
qe_{exp}	56.28	qe_{exp}	56.28
k_1	2.303×10^{-3}	k_2	1.6987
R^2	0.978	R^2	0.997

Table 4
The data of elemental analysis (%) of *P. animale* before and after ARP-2BX dye biosorption and only ARP-2BX dye.

Element (%)	ARP-2BX (Dye)	*Phormidium animale* (Before biosorption)	*Phormidium animale* (After biosorption)
C	46.44	7.23	50.4
H	6.97	1.86	7.17
N	6.30	0.07	5.75
O	40.29	90.84	36.68

dye removal rate. The dye biosorption rates declined by increasing initial dye concentrations. The increment of biosorbent (dried *P. animale*) dosage (up to 4 g/L) resulted in augmentation of biosorption rate up to 97.35 ± 0.65% at 25 °C. The biosorption rate of ARP-2BX dye by dried *P. animale* increased to 99.70 ± 0.27% with the increment of temperature up to 45 °C. The results of FTIR, elemental analysis and biosorption isotherms and kinetics concluded that *P. animale* was a favorable biosorbent for treatment of textile wastewater.

Declarations of Competing Interest

None

References

Aksu, Z., Tezer, S., 2005. Biosorption of reactive dyes on the green alga *Chlorella vulgaris*. Process Biochem. 40, 1347–1361.

Aravindhan, R., Rao, J.R., Nair, B.U., 2007. Removal of basic yellow dye from aqueous solution by sorption on green alga *Caulerpa scalpelliformis*. J. Hazard. Mater. 142, 68–76.

Bilal, M., Rasheed, T., Sosa-Hernández, J.E., Raza, A., Nabeel, F., Igbal, H.M.N., 2018. Biosorption: an interplay between marine algae and potentially toxic elements—a review mar. Drugs 16, 65),1–16.

Celekli, A., Yavuzatmaca, M., Bozkurt, H., 2009. Kinetics and equilibrium studies on the adsorption of reactive red 120 from aqueous solution on Spirogyra majuscule. Chem. Eng. J. 152, 139–145.

Chen, X., Liu, T., Wang, Q., 2014. The growth of Scenedesmus sp. attachment on different materials surface. Microb. Cell Fact. 13, 142.

Chia, M.A., Musa, R.I.I., 2014. Effect of indigo dye effluent on the growth, biomass production and phenotypic plasticity of *Scenedesmus quadricauda chlorococcales*. An. Acad. Bras. Cienc. 86, 419–428.

Dotto, G.L., Vieira, M.L.G., Esquerdo, V.M., Pinto, L.A.A., 2013. Equilibrium and thermodynamics of Azo dyes biosorption onto Spirulina platensis. Braz. J. Chem. Eng. 30, 13–21.

Elumalai, S., Saravan, G.K., 2016. The role of microalgae in textile dye industrial waste water recycle (Phycoremediation). Int. J. Pharm. Bio. Sci. 7, 662–673.

Ertuğrul Karatay, S., Dönmez, G., Aksu, Z., 2017. Effective biosorption of phenol by the thermophilic cyanobacterium *Phormidium* sp. Water Sci. Technol. 76, 3190–3194.

Freundlich, H., 1906. Adsorption in solution. Phys. Chem. Soc. 40, 1361–1368.

Helfferich, F., 1962. Ion Exchange. McGraw Hill, New York, USA, p. 166.

Ip, P.F., Chen, F., 2005. Production of astaxanthin by the green microalga *Chlorella zofingiensis* in the dark. Process Biochem. 40, 733–738.

Kenney, J., Keeping, E.S., 1951. Standard Error of the Mean. In: Princeton, N., Nostrand, V. (Eds.), Mathematics of Statistics, vol. 110, pp. 132–133.

Kousha, M., Daneshvar, E., Sohrabi, M.S., Koutahzadeh, N., Khataee, A.R., 2012. Optimization of C.I. acid black 1 biosorption by *Cystoseira indica* and *Gracilaria persica* biomasses from aqueous solutions. Int. Biodeter. Biodegr. 67, 56–63.

Langmuir, I., 1918. The adsorption of gases on plane surfaces of glass, mica, and platinum. J. Am. Chem. Soc. 40, 1361–1368.

Lim, S.-L., Chu, W.-L., Phang, S.-M., 2010. Use of *Chlorella vulgaris* for bioremediation of textile wastewater. Bioresour. Technol. 01, 7314–7322.

Mane, P.C., Bhosle, A.B., Deshmukh, P.D., Jangam, C.M., 2010. Chromium adsorption on activated carbon derived from tendu (diospyros melanoxylon) leaf refuse: influence of metal/carbon ratio, time and pH. Adv. Appl. Sci. Res. 1, 212–221.

Marungrueng, K., Pavasant, P., 2006. Removal of basic dye (Astrazon blue FGRL) using macroalga *Caulerpa lentillifera*. J. Environ. Manage. 78, 268–274.

Michalak, I., Chojnacka, K., Witek-Krowiak, A., 2013. State of the art for the biosorption process - a review. Appl. Biochem. Biotechnol. 170, 1389–1416.

Mnif, I., Fendri, R., Ghribi, D., 2015. Malachite green bioremoval by a newly isolated strain *Citrobacter sedlakii* RI11; enhancement of the treatment by biosurfactant addition. Water Sci. Technol. 72, 1283–1293.

Mnif, I., Maktouf, S., Fendri, R., Kriaa, M., Ellouze, S., Ghribi, D., 2016. Improvement of methyl orange dye biotreatment by a novel isolated strain, *Aeromonas veronii* GRI, by SPB1 biosurfactant addition. Environ. Sci. Pollut. Res. 23, 1742–1754.

Mona, S., Kaushik, A., Kaushik, C.P., 2011. Biosorption of reactive dye by waste biomass of *Nostoc linckia*. Ecol. Eng. 37, 1589–1594.

Omar, H., El-Gendy, A., Al-Ahmary, K., 2018. Bioremoval of toxic dye by using different marine macroalgae. Turk. J. Bot. 42, 15–27.

Ozer, A., Akkaya, G., Turabik, M., 2005. Biosorption of acid red 274 on *Enteromorpha prolifera* in a batch system. J. Hazard. Mater. 126, 119–127.

Preeti, K., Veena, S., 2017. Bioremediation of textile dyes by using blue green algae. Int. J. Sci. Res. Dev. 5, 1322–1324.

Renuka, N., Sood, A., Prasanna, R., Ahluwalia, A.S., 2014. Influence of seasonal variation in water quality on the microalgal diversity of sewage wastewater. S. Afr. J. Bot. 90, 137–145.

Rippka, R., 1988. Isolation and purification of cyanobacteria. Methods Enzym. 167, 3–27.

Sadegh, H., Mazloumbilandi, M., Chahardouri, M., 2017. Low-cost materials with adsorption performance. In: Martínez, L., Kharissova, O., Kharisov, B. (Eds.), Handbook of Ecomaterials. Springer, Cham, pp. 1–33.

Salvi, N.A., Chattopadhyay, S., 2017. Biosorption of Azo dyes by spent *Rhizopus arrhizuss* biomass. Appl. Water Sci. 7, 3041–3054.

Tastan, B.E., Tekinay, T., 2016. A novel coal additive from microalgae produced from thermal power plant flue gas. J. Clean. Prod. 133, 1086–1094.

Theivandran, G., Mohamed Ibrahim, S., Murugan, M., 2015. Fourier transform infrared (Ft-IR) spectroscopic analysis of *Spirulina Fusiformis*. J. Med. Plants Studies 3, 30–32 .

Tunalı Akar, S., Celik, S., Tunc, D., Yetimoglu, Y., Akar, T., 2016. Biosorption potential of surface-modified waste sugar beet pulp for the removal of reactive yellow 2 (RY2) anionic dye. Turk. J. Chem. 40, 1044–1054.

Yaseen, D.A., Scholz, M., 2018. Treatment of synthetic textile wastewater containing dye mixtures with microcosms. Environ. Sci. Pollut. Res. Int. 25, 1980–1997.